Crystallinity and surface effects on Young's modulus of CuO nanowires

E. P. S. Tan
Division of Bioengineering, Department of Mechanical Engineering, National University of Singapore, Singapore 117576, Singapore

Y. Zhu
NUS Nanoscience and Nanotechnology Initiative, National University of Singapore, Singapore 117576, Singapore and Department of Physics, National University of Singapore, Singapore 117542, Singapore

T. Yu
Division of Physics and Applied Physics, Nanyang Technological University, Singapore 637616, Singapore

L. Dai
NUS Nanoscience and Nanotechnology Initiative, National University of Singapore, Singapore 117576, Singapore

C. H. Sow
NUS Nanoscience and Nanotechnology Initiative, National University of Singapore, Singapore 117576, Singapore and Department of Physics, National University of Singapore, Singapore 117542, Singapore

V. B. C. Tan and C. T. Lim[a)]
Division of Bioengineering, Department of Mechanical Engineering, National University of Singapore, Singapore 117576, Singapore and NUS Nanoscience and Nanotechnology Initiative, National University of Singapore, Singapore 117576, Singapore

(Received 8 January 2007; accepted 16 March 2007; published online 18 April 2007)

The authors investigate the crystallinity and surface effects on Young's modulus of cupric oxide (CuO) nanowires by performing three-point bend test using atomic force microscopy. Young's modulus of the nanowires obtained ranges from 70 to 300 GPa and is dependent on two factors. Firstly, it depends on whether the nanowire is mono- or polycrystalline, as indicated by the absence or presence of an amorphous surface layer. Second, the modulus increases with decreasing diameter for both types of nanowires. Combined with transmission electron microscopy and computational simulation studies, the nanostructure-mechanical property relationship of CuO nanowires is elucidated. © *2007 American Institute of Physics*. [DOI: 10.1063/1.2723654]

As a *p*-type semiconductor, cupric oxide (CuO) attracted much interest because of its important role in building high-temperature superconductors.[1,2] Recently, the nanowire form of CuO has attracted attention due to its potential use as an electron field emission source.[3] Techniques developed to produce CuO nanowires include vapor-solid reaction[3–5] and a combination of electrodeposition and self-catalytic growth.[6] Many techniques have been used to characterize the fundamental properties of CuO such as chemical, structural and electrical properties. However, in order to fully assess the functionality of the nanowires in potential applications such as in nanoelectromechanical system/microelectromechanical system, there is also a need to evaluate the mechanical properties of individual CuO nanowires. This letter investigates the mechanical properties of single CuO nanowires using atomic force microscopy (AFM). A nanoscale three-point bend test is performed and Young's modulus of the nanowire obtained. The nanostructure-mechanical property relationship is also established based on the nanostructural makeup of the nanowires obtained using transmission electron microscopy (TEM). Computational simulations were carried out to compare with that of experimental results obtained from the three-point bend test.

CuO nanowires were prepared using the vapor-solid reaction method as detailed in our previous studies.[3,4] A copper plate was heated to 400 °C under ambient conditions until a black layer was formed on the substrate. This layer was peeled off and put in de-ionized water. After ultrasonic agitation, some nanowires detached from the substrate and suspended freely in de-ionized water. Several drops of the nanowire-water suspension were deposited on Cu grids and air dried for TEM (JEOL, JEM-2010F, 200 kV) study. A few drops of the suspension were deposited onto a silicon AFM calibration grid with 200 nm deep and 5 μm wide square holes for three-point bend test. As-fabricated CuO nanowires have diameters ranging from tens to a few hundreds of nanometers and lengths up to 50 μm. Most nanowires have a larger diameter at the base (portion of the nanowire attached to the substrate) but sharper at the tips.[3] After ultrasonic agitation, the as-fabricated nanowires are broken down to segments of several micrometers in length.

Some nanowires deposited on the AFM calibration grid span across the holes as shown by the circles in Fig. 1(a). The nanowires can have a tapered or uniform cross section as shown in Figs. 1(b) and 1(c), respectively. Nanowires are considered uniform when the percentage difference in diameter between the two ends of the nanowires is below 10% and tapered otherwise. A preliminary survey of the nanowires under a scanning electron microscope revealed that tapered nanowires may have rougher surfaces than that of uniform nanowires. Thus, the surface roughness of the nano-

[a)]Author to whom correspondence should be addressed; FAX: (65)67791459; electronic mail: ctlim@nus.edu.sg

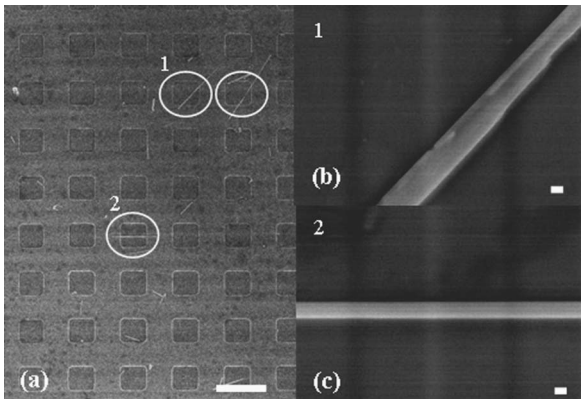

FIG. 1. Scanning electron microscopy images of CuO nanowires deposited on AFM calibration grid. (a) Nanowires spanning across holes, (b) close-up image of tapered nanowire as indicated by 1 in (a) and (c) close-up image of uniform nanowire as indicated by 2 in (a). The scale bars represent 10 μm in (a) and 100 nm in (b) and (c).

wires was measured using an AFM (Dimension 3100, Digital Instruments) by imaging an area of 50×50 nm^2 using the tapping mode of AFM. The root-mean-square roughness measured was found to be independent of the nanowire diameter, which ranged from 80 to 215 nm in this study.

Figure 2 shows the high resolution TEM (HRTEM) images of CuO nanowires. There is an amorphous layer (~5 nm) covering the cylindrical body of the CuO nanowire in Fig. 2(a), whereas this layer is almost absent for some other nanowires [Fig. 2(b)]. This layer could have been formed during the cooling-down process after growth with the thickness varying along the wire and between wires. In ideal situations, the CuO nanowire core is single crystal as shown by the clear lattice fringes in Fig. 2 and Ref. 3. Here, the lattice spacing was measured to be about 2.5 Å, matching the (110) interface spacing of monoclinic CuO structures.[7] The wire axis is parallel to the $[\bar{1}11]$ direction of CuO crystal. As the nanowires are produced by simply heating a piece of Cu in air, the details of local conditions during growth such as variations in temperature and oxygen content and the surface roughness of Cu could give rise to both clean or amorphous-cladded nanowires on the same piece of Cu. Furthermore, this may also result in some nanowires having imperfect crystals or polycrystalline structures. This is supported by several HRTEM images showing that nanowires with an amorphous layer appear to have rough surfaces whereas nanowires without this layer show very smooth surfaces. The amorphous material is made up of CuO based on Raman spectroscopy and energy dispersive x-ray analysis.

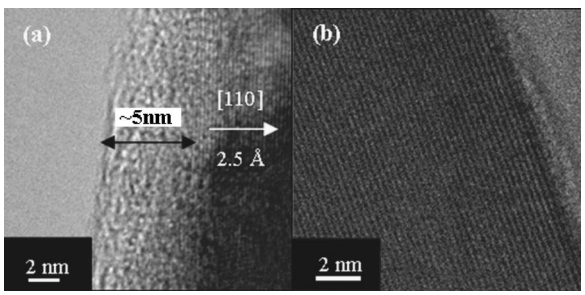

FIG. 2. HRTEM images of as-grown CuO nanowires showing (a) the presence of amorphous layer and (b) the absence of amorphous layer.

Three-point bend test of a single suspended nanowire was performed using AFM by applying a point load at the midspan of the nanowire using an AFM tip. This method of obtaining Young's modulus has been used on carbon nanotubes,[8] polymeric nanofibers,[9,10] and metallic nanowires.[11] AFM cantilevers with spring constants in the range of 0.57–3.3 N m^{-1} were used to apply a maximum loading force of 40–90 nN at a loading rate of 1.6–3.0 μm s^{-1}. The method proposed by Torii *et al.*[12] was used to measure the spring constant of the cantilevers. Five to seven force curves were obtained from each sample at the midspan.

Young's modulus (E) for both uniform and tapered nanowires is calculated based on beam bending theory[13] for a three-point bend test of a beam with two ends fixed and is given as

$$E = \frac{FL^3}{192\delta I}, \tag{1}$$

where F is the maximum force applied, L is the suspended length, δ is the deflection of the beam at the midspan, and I is the second moment of area (where $I=\pi D^4/64$ and D is the beam diameter). The method of obtaining the above variables experimentally can be found in another study.[10]

Computational simulations were carried out to investigate the elastic properties of the single crystal CuO via CASTEP, a package coded with density functional theory.[14] Plane-wave functions were used at a cutoff energy of 400 eV, ultrasoft pseudopotentials and Perdew-Burke-Ernzerhof forms of generalized gradient approximations were selected for the atomic cores and electron-exchange-correlation functions.[15] The simulated equilibrium state of the monoclinic CuO single crystal structure[16] agreed well with our experimental observations with less than 0.5% error on the cell parameters and atomic positions. Elastic modulus in the $[\bar{1}11]$ crystal direction and Young's modulus for the bulk polycrystalline phase were computed in order to make comparison with experimental results.

Based on the optimized structure, the elastic constants, c_{ij}, with respect to various strain conditions, were calculated as the second derivatives of the energy density

$$C_{ij} = \frac{1}{V}\left(\frac{\partial^2 U}{\partial\varepsilon_i\partial\varepsilon_j}\right), \tag{2}$$

where V is the crystal volume, U is the total energy, and ε_{ij} is the strain in directions i and j. The elastic modulus was calculated as 170 GPa in the $[\bar{1}11]$ crystal direction with the crystal axis rotated.

The theory of Hashin-Shtrikman (HS) was employed to obtain the mechanical properties of polycrystalline CuO.[17] The HS theory considers the material as composed of spheres of grains with various sizes and concentrations, and uses the elastic constants c_{ij} to compute the bulk mechanical properties. Young's modulus of monoclinic CuO bulk phase was obtained as 81.6 GPa.

Figure 3 shows results of the three-point bend test as a plot of Young's modulus against the average diameter of the nanowire for both uniform and tapered nanowires. Young's modulus of single CuO crystal in the $[\bar{1}11]$ direction and polycrystalline CuO obtained from simulation are indicated in the figure. It can be seen from Fig. 3 that uniform nano-

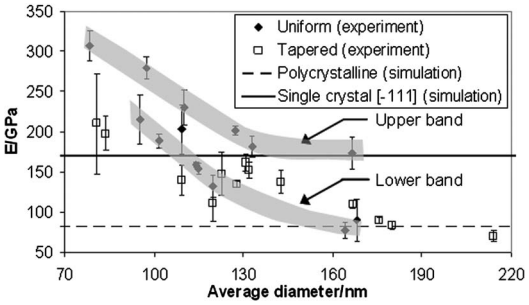

FIG. 3. Variation of Young's modulus with nanowire diameter for uniform and tapered nanowires. Single and polycrystalline CuO properties are from the simulation results. Young's modulus of uniform nanowires is divided into upper (low average surface roughness of 0.75 nm) and lower (high average surface roughness of 1.46 nm) bands.

wires have Young's modulus that is divided into two bands as indicated by the curves. Two observations can be made from the graph. First, the nanowires appear to be divided into two types; one indicated by the upper band which consists of uniform nanowires with low average surface roughness of 0.75 nm, and the other indicated by the lower band which consists of uniform nanowires with higher average surface roughness of 1.46 nm and tapered nanowires with comparable surface roughness of 1.31 nm. Second, Young's modulus of both types of nanowires displays diameter dependence, i.e., the modulus value increases as the diameter decreases below a certain size of about 180 nm.

The first observation suggests that uniform wires with smooth surface have a different structure or composition from uniform wires with rough surface as well as the tapered wires. Nanowires in the upper band have modulus that approaches the value for single CuO crystal in the $[\bar{1}11]$ direction for diameters larger than 130 nm. Nanowires in the lower band have modulus that approaches the value for polycrystalline CuO for diameters larger than 170 nm. Thus it can be deduced that smooth nanowires with uniform diameter have a perfect single crystal structure and an absence of surface amorphous layer. Nanowires with rough surface, regardless of shape, most likely have an amorphous surface layer and imperfect crystal structure or different crystal orientations within the same wire. The scatter of results in the lower band could be due to various crystal orientations or number of crystals that exist in each nanowire. As the volume of amorphous content can occupy up to 25% of the total nanowire volume (assuming amorphous layer ~5 nm and wire diameter ~80 nm), this layer may contribute to the lower modulus observed in the lower band. However, based on the strong agreement of experimental and computational simulation results, the most likely reason for the separation of the modulus values into two bands is the variation in the core structure of the nanowires.

The second observation of diameter dependence could be due to the presence of fewer defects in smaller wires with diameter ranging from tens to hundreds of nanometers, as reported in other studies.[9] However, this may unlikely be the predominant factor as Young's modulus is known to be rather insensitive to defect concentration.[18] The more likely reason could be the fact that surface effects become significant due to a dramatic increase in surface area to volume ratio as the nanowire diameter decreases.[18,19] Cuenot *et al.*[18] proposed that as the nanowire is deformed, an increase in surface area is induced and thus surface tension effects may account for the observed diameter dependence. They proposed that the surface tension or surface stress is more predominant in nanomaterials as the surface area to volume ratio increases dramatically. In a study by Chen *et al.*[19] on the size dependence of Young's modulus in ZnO nanowires, they proposed that the surface atoms have imperfect coordination number, which causes the remaining bonds of the lower coordinated surface atoms to relax and raises the binding energy. As a result, more energy is required to deform the surface layers of atoms, which could be the predominant factor in nanowires with smaller diameter.

In summary, nanoscale three-point bend test using AFM was carried out to evaluate Young's modulus of CuO nanowires produced by the vapor-solid reaction method. TEM study and computational simulations were also conducted. The modulus of the nanowires ranged from 70 to 300 GPa and is divided into two bands. The modulus of large nanowires in the upper and lower band was found to be the same as the modulus of single CuO crystal in the $[\bar{1}11]$ direction and polycrystalline CuO, respectively. The surface roughness of nanowires is a good indicator of the absence or presence of amorphous layer and the core structure within. The modulus of both types of nanowires increased as the diameter decreased due to the increase in surface effect for smaller wires.

This work was supported by the Science and Engineering Research Council (SERC) of the agency for Science, Technology and Research (A*STAR).

[1] M. K. Wu, J. R. Ashburn, C. J. Torng, P. H. Hor, R. L. Meng, L. Gao, Z. J. Huang, Y. Q. Wang, and C. W. Chu, Phys. Rev. Lett. **58**, 908 (1987).
[2] H. He, P. Bourges, Y. Sidis, C. Ulrich, L. P. Regnault, S. Pailhes, N. S. Berzigiarova, N. N. Kolesnikov, and B. Keimer, Science **295**, 1045 (2002).
[3] Y. W. Zhu, T. Yu, F. C. Cheong, X. J. Xu, C. T. Lim, V. B. C. Tan, J. T. L. Thong, and C. H. Sow, Nanotechnology **16**, 88 (2005).
[4] T. Yu, X. Zhao, Z. X. Shen, Y. H. Wu, and W. H. Su, J. Cryst. Growth **268**, 590 (2004).
[5] T. Yu, C. H. Sow, A. G. Mahapatruni, F. C. Cheong, Y. W. Zhu, K. C. Chin, X. Xu, C. T. Lim, Z. X. Shen, J. T. L. Thong, and A. T. S. Wee, Nanotechnology **16**, 1238 (2005).
[6] C.-T. Hsieh and J.-M. Chen, Appl. Phys. Lett. **82**, 3316 (2003).
[7] In Joint Committee on Powder Diffraction Standards, Diffraction Data File No. 45–0937 [International Centre for Diffraction Data (ICDD, formerly JCPDS), Newtown Square, PA, 1991].
[8] J.-P. Salvetat, J.-M. Bonard, N. H. Thomson, A. J. Kulik, L. Forro, W. Benoit, and L. Zuppiroli, Appl. Phys. A: Mater. Sci. Process. **69**, 255 (1999).
[9] S. Cuenot, S. Demoustier-Champagne, and B. Nysten, Phys. Rev. Lett. **85**, 1690 (2000).
[10] E. P. S. Tan and C. T. Lim, Appl. Phys. Lett. **84**, 1603 (2004).
[11] B. Wu, A. Heidelberg, and J. J. Boland, Nat. Mater. **4**, 525 (2005).
[12] A. Torri, M. Sasaki, K. Hane, and S. Okuma, Meas. Sci. Technol. **66**, 179 (1996).
[13] A. C. Ugural, *Mechanics of Materials* (McGraw-Hill, Singapore, 1993), pp. 152–213.
[14] S. J. Clark, M. D. Segall, C. J. Pickard, P. J. Hasnip, M. J. Probert, K. Refson, and M. C. Payne, Z. Kristallogr. - New Cryst. Struct. **220**, 567 (2005).
[15] C. Lee, W. Yang, and R. G. Parr, Phys. Rev. B **37**, 785 (1988).
[16] G. V. Samsonov, *The Oxide Handbook*, 2nd ed. (IFI/Plenum Data, New York, 1982), p. 10.
[17] G. F. Davies and J. O'Connell, Rev. Geophys. Space Phys. **14**, 541 (1976).
[18] S. Cuenot, C. Fretigny, S. D. Champagne, and B. Nysten, Phys. Rev. B **69**, 165410 (2004).
[19] C. Q. Chen, Y. Shi, Y. S. Zhang, J. Zhu, and Y. J. Yan, Phys. Rev. Lett. **96**, 075505 (2006).